Surface Wave Anisotropy in Fractured Media

Insights from Wavefield Modelling and Applications for Geothermal Exploration

Kennedy, H.; Finger, C.; Löer, K.; Gilligan, A.

DOI
10.3997/2214-4609.2024101344

Publication date
2024

Document Version
Final published version

Citation (APA)
Kennedy, H., Finger, C., Löer, K., & Gilligan, A. (2024). *Surface Wave Anisotropy in Fractured Media: Insights from Wavefield Modelling and Applications for Geothermal Exploration* . Paper presented at 85th EAGE Annual Conference & Exhibition 2024, Oslo, Lillestrøm, Norway. https://doi.org/10.3997/2214-4609.2024101344

Surface Wave Anisotropy in Fractured Media: Insights from Wavefield Modelling and Applications for Geothermal Exploration

H. Kennedy[1], C. Finger[3], K. Löer[2], A. Gilligan[1]

[1] University of Aberdeen; [2] Delft University of Technology; [3] Fraunhofer Institution for Energy Infrastructures and Geothermal Systems

Summary

Characterizing faults in geothermal fields is essential for the energy transition, as faults enable efficient heat flow throughout the reservoir. Three-component (3C) beamforming, an ambient seismic noise technique, is a cheap and effective way to analyse fault-related anisotropy by observing surface wave velocities. 3C beamforming extracts the wave type, direction and phase velocities of coherent waves as a function of frequency, which provides an understanding of surface wave velocities. Anisotropic velocities have been shown to be caused by the presence of faults, giving an indication of the maximum depth of permeability within a geothermal reservoir. However, the relationship between faults and surface wave velocities must be examined in more detail. Wavefield modelling using a numerical model was done by propagating a wave through a model of the subsurface with anisotropy applied in the form of a fault at assumed directions. 3C beamforming was then used to analyse this synthetic data, providing information on an identifiable Rayleigh wave and how the velocity of the wave changes depending on fault azimuth. Therefore, indicating the effectiveness of ambient noise methods, like 3C beamforming, compared to that of far more expensive active seismic techniques; the development of which is crucial for the energy transition.

Surface Wave Anisotropy in Fractured Media: Insights from Wavefield Modelling and Applications for Geothermal Exploration

Introduction

Fault characterization is crucial for further developing geothermal fields for the energy transition; faults and fractures provide secondary permeability, thus are essential parameters in geothermal exploration. This study used three-component (3C) beamforming of ambient seismic noise (B3AM; a cheaper, widely available method suitable for monitoring) to analyse fault-related anisotropy in surface wave velocities. We use wavefield modelling to gain further insight into the behaviour of Rayleigh waves in fractured media and the implications for applying B3AM in these situations.

3C beamforming, as devised by Riahi et al. (2013), is an array-based method that extracts the polarizations (wave type), azimuths (direction), and phase velocities of coherent waves as a function of frequency, providing a detailed understanding of surface wave velocities at different azimuths and depths (Kennedy et al., 2022). Anisotropic velocities can be caused by the presence of faults, indicating the maximum permeability depth essential for fluid circulation and heat flow throughout a geothermal field, for example. However, our analysis suggests that certain structures/features substantially affect surface wave velocity more than others (Kennedy et al., 2022).

To enable a robust interpretation of the B3AM results, this relationship needs to be examined in more detail using numerical simulation of wave propagation through a model of the subsurface with anisotropy applied in the form of faults/fractures at assumed directions. B3AM is then used on the synthetic seismic data: Observations of the maximum beam energy and corresponding polarization of the synthetic data will indicate the dominant wavefield component (Rayleigh, Love or body wave) in a given time window. Hence, it allows for an identifiable Rayleigh wave within a given time window to be recognised, which enables the analysis of its azimuth and velocity. Comparing the true and the measured anisotropy of Rayleigh waves allows for investigating the effect of fault parameters on the observed anisotropy and its recoverability with B3AM. Therefore, it is essential to understand better how B3AM identifies velocity changes of a Rayleigh wave relevant to the angle of a fault and how these changes are based on the proposed reservoir geology. We will show the results of an identifiable retrograde Rayleigh wave, the velocity changes due to anisotropic differences and relate that to our understanding of past behaviours with real ambient noise data.

Method and Theory

Three-component Beamforming

B3AM can identify different waves because of their polarization; their particle motion at the surface (Löer et al., 2018). Rayleigh waves are described as an ellipse in the vertical plane, parallel or antiparallel to the direction of propagation (Riahi et al., 2013). If anisotropy exists, waves travelling in different directions will have different propagation velocities; anisotropic media cause the observed apparent anisotropy and can be biased by the used array design; tests have been done in the past to check this as well as accounting for array effects on azimuth (this can be observed with an array response function (Kennedy et al., 2022)). Fig.1 shows the variation in apparent anisotropy of passive seismic data from the Los Humeros Geothermal Field in Mexico. The surface waves identified in the ambient noise wavefield were analysed at discrete frequencies and in short time windows individually, which were thus then combined into a histogram (Fig.1) (Kennedy et al., 2022). Anisotropy parameters (Equation 1) were then fitted to the velocity versus azimuth histograms for both Love and Rayleigh waves (Kennedy et al., 2022); retrograde Rayleigh waves are the focus of the analysis due to their greater depth permeability.

$$v(\theta) = a_0 + a_1 cos(2\theta) + a_2 sin(2\theta) + a_3 cos(4\theta) + a_4 sin(4\theta) \quad (1)$$

Observations of the anisotropy curves can be used to make assumptions on subsurface structures. Kennedy et al. (2022) claim that the fast velocities of retrograde Rayleigh waves correspond to the orientation of faults and/or fractures based on the assumption that Rayleigh waves travel faster when running parallel along a fault rather than perpendicular to the fault. Anisotropic velocities in low frequency Rayleigh waves could indicate that hydrothermal faults continue at depth. Therefore, we use a numerical model to

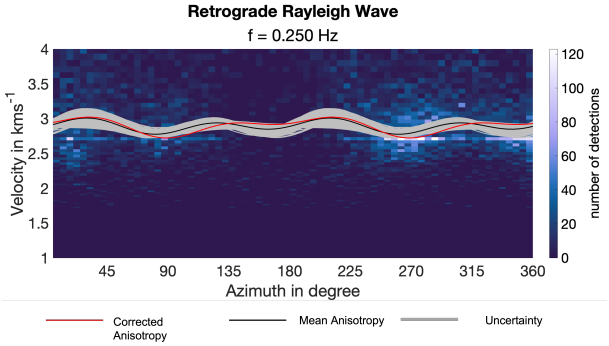

Figure 1: Histogram showing the apparent anisotropy curve, change in velocity vs azimuth, of a Retrograde Rayleigh wave of a frequency of 0.25 Hz. Number of detections (color bar), anisotropy corrected for the array effect (red line), mean anisotropy (black line), uncertainty of mean anisotropy (grey area) (Kennedy et al., 2022).

investigate Rayleigh wave velocities at different angles across a fault in an otherwise isotropic medium.

Wavefield Modelling

We employed a rotated staggered grid (RSG) - finite difference (FD) scheme (Saenger et al., 2000), which can be used for modelling wave propagation in elastic anisotropic media (Krüger et al. (2005), Saenger et al. (2000)); we focus on elastic, isotropic simulations that include anisotropy through the geometry of the fault. Using the RSG-FD scheme, a homogeneous half-space with a vertical fault-like structure (140 m width in total including surrounding "damage-zone", overall fault-to-wavelength ratio based on real scale ratio in LHGF in Mexico) was modelled. A three-dimensional (3D) model was used, 100 x 200 x 200 grid points (gdpts), with a grid spacing of 20 m (Δx), making the model 2 x 4 x 4 km in dimension; there is also a free surface at the top of the model with parameters of that of a vacuum to simulate the surface, as we need a free surface to create and simulate surface waves. Absorbing boundary conditions were applied, and the model's total time was 7.2 s, with a time step (Δt) of 0.0009 s, and the frequency range used for beamforming analysis was 1 to 3 Hz. Two scenarios were used; one had the same geological parameters as the LHGF, and the other mimicked the geology of geothermal fields in production in Cornwall, UK (Table: 1). An overall average for the surrounding rock and fault 'fill' was used based on the literature of other geological studies; it is rather homogeneous for the sake of wavefield complexity, which is kept to a minimum to be able to observe the effect of the faults visually. These faults in their respective geological conditions were then rotated to different angles to see the effect of the azimuth on the velocity of the identifiable Rayleigh wave.

Geological Sceanarios	**Surrounding rock**			**Fault "fill"**		
	V_p	V_s	Rho	V_p	V_s	Rho
Cornwall, UK	3.000	1.500	1464	1.900	0.500	1660
LHGF, Mexico	3.000	1.500	2565	2.950	1.357	2039

Table 1: Parameters for the two geological scenarios used within the models, showing the compressional velocity (V_p), shear velocity (V_s) and density (rho) of both the surrounding rock and the "fill" of the fault. V_p and V_s in kms^{-1}, and rho in kgm^{-3}.

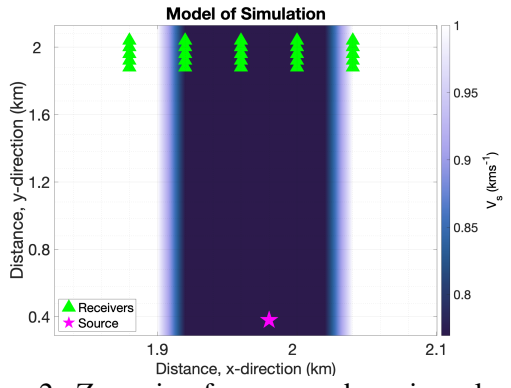

Figure 2: Zoom in of source and receivers layout, with a parallel fault ($\theta = 0°$) for the Cornwall simulation.

A single point source was used located at 0.4 km depth, 0.4 km from the South (y-direction) and 2 km East (x-direction), with a backazimuth of $-90°$ relative to the receiver array. 25 receivers were laid out in a regular rectangle; the minimum aperture is $d_{min} = 40m$, and the maximum aperture is $d_{max} = 230m$ (Fig.2). Considering a fundamental frequency of 3 Hz and Rayleigh wave velocities ($v_R = 0.9 * v_S$) between 0.45 kms^{-1} and 1.35 kms^{-1}, the expected wavelengths ($\lambda = v/f$) are in the range of 150 m to 450 m and hence within the recommendations by Tokimatsu et al. (1995) for array design: $\lambda_{max} < 3d_{max}$ and $\lambda_{min} > 2d_{min}$. Producing an isolated Rayleigh wave in a 3D model is challenging, as a large distance between source and receiver(s) is required for body and surface waves to separate, resulting in a large model and, hence, high computational costs. Within the model size manageable by the available HPC

cluster, this could not be achieved. Instead, the distance between the source and receiver array was chosen to be large enough for the wavefront to arrive at the receivers as a plane wave (1.5 km). At this distance, the recorded synthetic wavefield is a superposition of first arriving body waves (P and S) and slightly later Rayleigh waves (see Fig.3a). An example using a homogeneous model was first tested to prove an identifiable Rayleigh wave was produced and compared to anisotropy analysis.

Results

Our modelling results show how Rayleigh wave velocity changes as a function of the azimuth of the fault with respect to the wave propagation direction, allowing for anisotropic velocity comparisons to real data examples from Kennedy et al. (2022) using B3AM. Choosing the time window length in the beamformer carefully allows us to identify the different wavetypes and analyse the Rayleigh wave component only. Fig.3b shows the beam response for the time window indicated in (a): the polarization analysis (bottom) clearly identifies a retrograde Rayleigh wave, while the beam power plot (top) confirms the propagation direction of -90° (from South) at a wavenumber of just above 2 1/km (see red cross in both plots).
For each identified Rayleigh wave the velocity was calculated using $v_R = f_{fund}/k$, where $f_{fund} = 3Hz$ is the fundamental frequency and k is the wavenumber picked in the beam response. The velocities were confirmed by manually comparing the time shift of the Rayleigh wave arrival across the stations of the array. Fig.4 shows the measured velocities for different fault orientations (see azimuth on x-axis) using the geological parameters of both Cornwall (a) and Los Humeros (b); the same station layout has been used to mitigate the potential effect of the array design on the measured anisotropy. Azimuth is given with respect to wave propagation direction; that is, for 0^{-1} fault and wave propagation are parallel, and for 90^{-1} they are perpendicular.

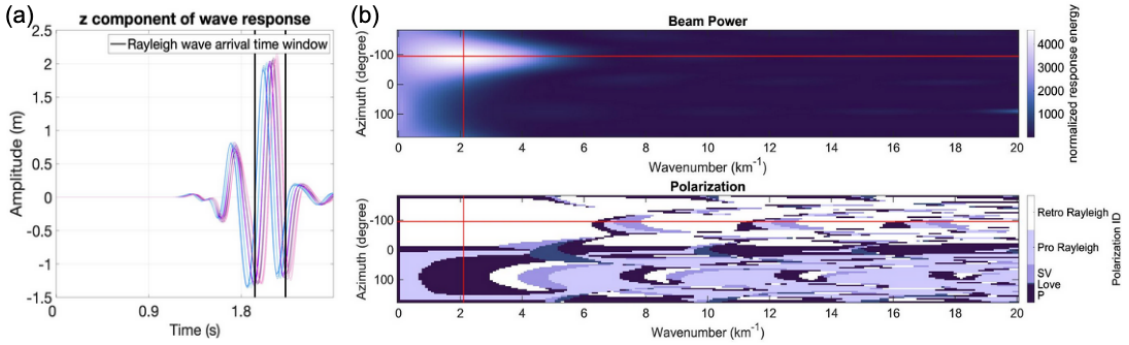

Figure 3: Example of an identified retrograde Rayleigh wave at 3 Hz for a simulation with a fault at 45°. (a) Time series showing the time window of the Rayleigh wave arrival (black lines, 2.32 s to 2.55 s) for all receivers (represented by different colour time series). (b) Normalised beam energy response, the maximum beam response corresponding to the source direction (top). The values for the maximum in the top plot (red cross) are used to pick the polarization ID (bottom), which, in this case, shows a retrograde Rayleigh wave in white.

Fig.4 shows the periodic variation in Rayleigh wave velocity as a function of fault angle (dots) compared to the homogeneous velocity (red line) for two different geological scenarios. In Cornwall (a) the largest deviation occurs at $\theta = 0°$, $\theta = 60°$ and $\theta = 120°$, where velocities drop to 1.38 kms^{-1} compared to 1.44 kms^{-1}, a change of 4%. For the LHGF (b) the results also show a periodic velocity variation with minima at $\theta = 0°$, $\theta = 60°$ and $\theta = 120°$, however, the deviation from the isotropic case is below 1%. The fastest velocities are measured at fault angles of $\theta = 30°$ and $\theta = 150°$.
Our results imply that the overall geological setting affects anisotropic surface wave propagation, and fault orientation is just one parameter amongst others to consider in the interpretation of field results. The results reflect the fact that the velocity contrast between fault "fill" and surrounding rock is much larger in the Cornwall setting than for LHGF, with the larger contrast causing larger magnitudes of anisotropy. In contrast to our hypothesis, we observe that in neither scenario does the fast direction coincide with the fault orientation. In fact, when the Rayleigh wave propagates along the fault ($\theta = 0°$), velocities are at a minimum, and the fast direction deviates by about $\theta = 30°$ from the fault orientation at LHGF, indicating that interpretation of anisotropy results might need a correction that is geology dependent.

Wave trapping in the fault and the affect of an isotropic array are further phenomena to be considered and investigated.

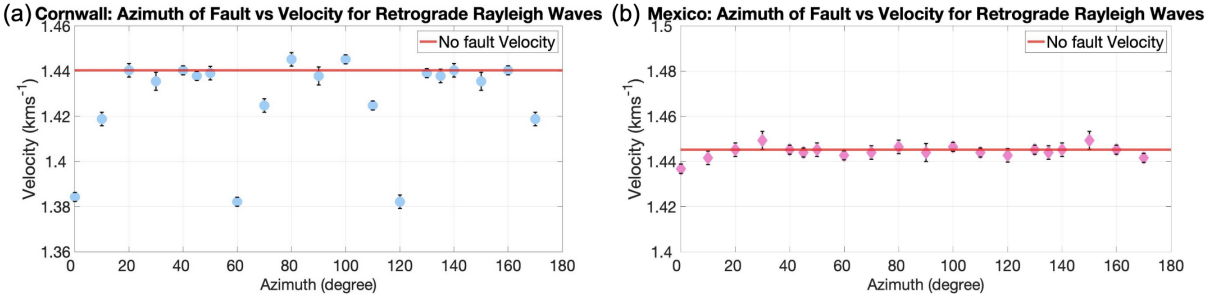

Figure 4: Velocity vs azimuth of fault for a retrograde Rayleigh wave 3 Hz for (a) Cornwall and (b) LHGF, Mexico, simulation. The error bars are the estimated error for the velocity calculation, and the red line is the velocity of the retrograde Rayleigh wave for a homogeneous model. Wave propagation is parallel to the fault for $\theta = 0^\circ$ and perpendicular for $\theta = 90^\circ$.

Conclusions

Three-component beamforming allows us to discriminate wavetypes in real and simulated seismic wavefields, providing vital information on surface wave velocities and propagation direction. Numerical models confirm that the presence and orientation of a fault are linked to anisotropic Rayleigh wave velocities, making them a valuable tool for fracture characterisation, for example, in geothermal fields. However, our results imply that the exact relationship is more complex than hypothesised and dependent on the overall geological setting. Additional numerical modelling will be required to assess the influence of different geological factors, such as magnitude of velocity contrast, fault size with respect to array aperture and dominant wavelength, or fault "fill" parameters. Considering the fractional costs of ambient noise methods like B3AM compared to active seismic techniques, their development will be crucial for the improved understanding of geothermal reservoirs and play a key role in the energy transition.

Acknowledgements

The work contained in this paper contains work conducted during a PhD study undertaken as part of the Centre for Doctoral Training (CDT) in Geoscience and the Low Carbon Energy Transition, and it is sponsored by the University of Aberdeen via their NERC GeoNetZero CDT Scheme, whose support is gratefully acknowledged. The interpretations and analyses were undertaken in the research facility at the University of Aberdeen, the underpinning financial and computer support for which is gratefully acknowledged. Furthermore, the modelling was conducted on the HPC Bochum cluster, the use and support of those affiliated with the cluster being gratefully acknowledged.

References

Kennedy, H., Löer, K. and Gilligan, A. [2022] Constraints on fracture distribution in the Los Humeros geothermal field from beamforming of ambient seismic noise. *Solid earth*, **13**(12), 1843–1858.

Krüger, O.S., Saenger, E.H. and Shapiro, S.A. [2005] Scattering and diffraction by a single crack: an accuracy analysis of the rotated staggered grid. *Geophysical Journal International*, **162**(1), 25–31.

Löer, K., Riahi, N. and Saenger, E.H. [2018] Three-component ambient noise beamforming in the Parkfield area. *Geophysical Journal International*, **213**(3), 1478–1491.

Riahi, N., Bokelmann, G., Sala, P. and Saenger, E.H. [2013] Time-lapse analysis of ambient surface wave anisotropy: A three-component array study above an underground gas storage. *Journal of Geophysical Research: Solid Earth*, **118**(10), 5339–5351.

Saenger, E.H., Gold, N. and Shapiro, S.A. [2000] Modeling the propagation of elastic waves using a modified finite-difference grid. *Wave motion*, **31**(1), 77–92.

Tokimatsu, K., Kōgakkai, J., of Soil Mechanics, I.S. and Foundation Engineering. TC4, E.G.E. [1995] *Geotechnical Site Characterization Using Surface Waves*.